

Geochemistry, Geophysics, Geosystems®



RESEARCH ARTICLE

10.1029/2022GC010529

Key Points:

- Coral luminescence green-to-blue ratio (coral G/B) is a quantitative proxy for terrigenous dissolved organic carbon concentration in river-influenced tropical coastal oceans
- Coral G/B can also be used to reconstruct the absorption spectrum of terrigenous chromophoric dissolved organic matter over the wavelength range 230–550 nm
- Downcore luminescence G/B variability can therefore be used to investigate temporal variability in terrigenous dissolved organic carbon input and its impacts on optical water quality

Supporting Information:

Supporting Information may be found in the online version of this article.

Correspondence to:

P. Martin,
pmartin@ntu.edu.sg

Citation:

Kaushal, N., Tanzil, J. T. I., Zhou, Y., Ong, M. R., Goodkin, N. F., & Martin, P. (2022). Environmental calibration of coral luminescence as a proxy for terrigenous dissolved organic carbon concentration in tropical coastal oceans. *Geochemistry, Geophysics, Geosystems*, 23, e2022GC010529. <https://doi.org/10.1029/2022GC010529>





Received 17 MAY 2022

Accepted 15 AUG 2022

Author Contributions:

Conceptualization: Patrick Martin
Data curation: Nikita Kaushal
Formal analysis: Nikita Kaushal, Jani T. I. Tanzil, Patrick Martin
Funding acquisition: Nikita Kaushal, Nathalie F. Goodkin, Patrick Martin

Environmental Calibration of Coral Luminescence as a Proxy for Terrigenous Dissolved Organic Carbon Concentration in Tropical Coastal Oceans

Nikita Kaushal^{1,2} , Jani T. I. Tanzil^{3,4}, Yongli Zhou^{1,5} , Maria Rosabelle Ong^{6,7}, Nathalie F. Goodkin^{1,7,8} , and Patrick Martin¹ 

¹Asian School of the Environment, Nanyang Technological University, Singapore, Singapore, ²Now at Department of Earth Sciences, Eidgenössische Technische Hochschule, Zürich, Switzerland, ³St. John's Island National Marine Laboratory, National University of Singapore, Singapore, Singapore, ⁴Tropical Marine Science Institute, National University of Singapore, Singapore, Singapore, ⁵Now at Marine Biological Laboratory, Woods Hole, MA, USA, ⁶Department of Earth and Environmental Sciences, Lamont-Doherty Earth Observatory, Columbia University, New York, NY, USA, ⁷Department of Earth and Planetary Sciences, American Museum of Natural History, New York, NY, USA, ⁸Earth Observatory of Singapore, Nanyang Technological University, Singapore, Singapore

Abstract The riverine flux of terrigenous dissolved organic matter (tDOM) to the ocean is a significant contributor to the global carbon cycle. In response to anthropogenic drivers the flux is expected to increase. This may impact the availability of sunlight in coastal ecosystems, and the seawater carbonate system and coastal CO₂ fluxes. Despite its significance, there are few long-term and high-resolution time series of tDOM parameters. Corals incorporate fluorescent tDOM molecules from the chromophoric dissolved organic matter (CDOM) pool in their skeletons. The resulting coral skeletal luminescence variability has traditionally been used to reconstruct hydroclimate variation. Here, we use two replicate coral cores and concurrent in-situ biogeochemical data from the Sunda Shelf Sea in Southeast Asia, where peatlands supply high tDOM inputs, to show that variability in coral luminescence green-to-blue ratios (coral G/B) can be used to quantitatively reconstruct terrigenous dissolved organic carbon (tDOC) concentration. Moreover, coral G/B can be used to reconstruct the CDOM absorption spectrum from 230 to 550 nm, and the specific ultraviolet absorbance at 254 nm (SUVA₂₅₄) of the DOM pool. Comparison to a core from Borneo shows that there may be site-specific offsets in the G/B–CDOM absorption relationship, but that the slope of the relationship is very similar, validating the robustness of the proxy. By demonstrating that corals can be used to estimate past changes in coastal tDOC and CDOM, we establish a method to study drivers of land–ocean tDOM fluxes and their ecological consequences in tropical coastal seas over decadal to centennial time scales.

Plain Language Summary Understanding the different processes of the carbon cycle is a critical priority to make increasingly accurate predictions of future CO₂ concentration. The riverine flux of dissolved organic carbon (DOC) to the coastal ocean may impact the availability of sunlight to coastal life forms, cause coastal water acidification and further degas to the atmosphere as CO₂. This DOC flux is particularly significant in regions with peatland soils with a high carbon content and where the flux is being further exacerbated by anthropogenic land-use changes. Despite this, there are few long-term instrumental measurements for DOC, and these are largely restricted to North America and Europe. In order to increase our understanding of the fate of DOC, we calibrate a method to reconstruct DOC records using luminescence measurements of coral cores. Coral skeletal luminescence is caused by the incorporation of humic acids, an integral component of terrestrial DOC. We use two replicate coral cores from coastal Singapore and concurrent biogeochemical measurements of coastal Singapore waters to show that coral luminescence measurements are quantitatively related to terrestrial DOC concentration measurements. Our proposed method can be used to reconstruct terrestrial DOC variability over centennial timescales allowing us to better understand the processes and consequences of its variability.

1. Introduction

The transfer of terrigenous Dissolved Organic Carbon (tDOC) from land to the coastal ocean is a significant flux in the global carbon cycle (Le Quéré et al., 2013). Tropical rivers contribute nearly two-thirds of the global land-to-ocean tDOC flux (Dai et al., 2012). Moreover, this flux appears to have been considerably perturbed

© 2022. The Authors.

This is an open access article under the terms of the [Creative Commons Attribution License](https://creativecommons.org/licenses/by/4.0/), which permits use, distribution and reproduction in any medium, provided the original work is properly cited.

Investigation: Nikita Kaushal, Jani T. I. Tanzil, Yongli Zhou, Maria Rosabelle Ong, Patrick Martin
Methodology: Nikita Kaushal, Jani T. I. Tanzil, Yongli Zhou, Nathalie F. Goodkin, Patrick Martin
Project Administration: Patrick Martin
Resources: Jani T. I. Tanzil, Nathalie F. Goodkin, Patrick Martin
Supervision: Patrick Martin
Validation: Nikita Kaushal, Jani T. I. Tanzil, Yongli Zhou, Maria Rosabelle Ong, Nathalie F. Goodkin, Patrick Martin
Visualization: Nikita Kaushal, Patrick Martin
Writing – original draft: Nikita Kaushal, Patrick Martin
Writing – review & editing: Nikita Kaushal, Jani T. I. Tanzil, Yongli Zhou, Maria Rosabelle Ong, Nathalie F. Goodkin, Patrick Martin

by human activity in recent times (Butman et al., 2015; Monteith et al., 2007; Noacco et al., 2017). Long-term increases in surface water DOC across North America and Europe are largely attributed to the recovery of ecosystems from historical atmospheric pollution (Monteith et al., 2007), although anthropogenic landscape alterations (Butman et al., 2015; Noacco et al., 2017) and climatic changes and permafrost thaw (de Wit et al., 2016; Larsen et al., 2011; Wauthy et al., 2018) are also implicated. In tropical regions, deforestation destabilizes soil organic carbon pools (Evans et al., 2014) and can lead to either net increases (Moore et al., 2013; Sanwlani et al., 2022) or net decreases (Drake et al., 2019) in riverine tDOC flux, depending on the lability of the newly mobilized soil carbon.

The environmental consequences of changing tDOC fluxes to the ocean depend on the biogeochemical fate of tDOC at sea, which remains poorly understood (Ciais et al., 2013). In parts of the Arctic and Southeast Asia, extensive remineralization of tDOC results in coastal seawater acidification and eventually degassing of CO₂ to the atmosphere (Wit et al., 2018; Zhou et al., 2021). tDOC is also rich in chromophoric dissolved organic matter (CDOM), which is that fraction of DOM that absorbs light. Increased fluxes of terrigenous CDOM can thus reduce underwater light availability and spectral quality in coastal waters (Urtizberea et al., 2013).

Despite the significance of tDOC and CDOM, long time series of their fluxes and concentrations in coastal waters are only available in parts of Europe and North America. Although CDOM and DOC can be estimated by satellite remote sensing (Liu et al., 2019; Sanwlani et al., 2022; Signorini et al., 2019) accurate remote sensing in optically complex coastal waters requires extensive optical and biogeochemical field data for algorithm development, which limits the widespread use of this technique. Moreover, satellite remote sensing can only provide data over the most recent few decades. Longer records are required to understand the impact of anthropogenic changes that pre-date the satellite era, as well as long-term and cyclical drivers of terrigenous CDOM and tDOC variability such as temperature and hydrology. It is therefore necessary to find a paleoproxy to reconstruct terrigenous dissolved organic matter (tDOM) parameters.

In the absence of measured instrumental records, we look to natural archives such as corals for geochemical paleoproxies. Corals offer exceptional chronological constraints and allow for approximately monthly resolution climate and environmental proxy reconstruction over hundreds of years (Thompson, 2022 and references therein). It has long been known that skeleton cores from corals such as *Porites* spp., composed of the calcium carbonate polymorph aragonite, show luminescent layers under UV light (Isdale, 1984). The luminescence intensity of these bands correlates with freshwater run-off over decadal and centennial time-scales, as shown in multiple locations including Australia (Lough, 2007; Rodriguez-Ramirez et al., 2014), Florida Bay (Smith et al., 1989) and Madagascar (Grove et al., 2013).

The luminescence is caused by the incorporation of humic-like substances into the coral skeleton during growth (Kaushal et al., 2020; Susic et al., 1991). Humic-like substances on land are formed from the breakdown of plant tissue, and after leaching into aquatic ecosystems they form an integral component of terrigenous CDOM and tDOC. Humic-like substances are rich in fluorescent aromatic moieties, and this fluorescence extends to longer wavelengths than that of coral skeletal aragonite. Therefore, when a coral core is illuminated with ultraviolet light, the ratios of emitted luminescence in the green wavelength band to that in the blue wavelength band (G/B ratio) measures downcore variability in the concentration of terrigenous humic-like substances, while normalizing for luminescence variation caused by changing coral skeletal structure (Grove et al., 2010; Kaushal et al., 2020). Moreover, we recently showed that luminescence G/B in a coral from Borneo, extending back to 2002, tracks sub-annual terrigenous CDOM variability, as estimated from satellite-based measurements of the CDOM absorption coefficient at 440 nm (Kaushal et al., 2021). While luminescence G/B thus clearly has high potential as a paleoproxy for tDOM, reconstructing just CDOM absorption at a single wavelength from a coral core can only give limited insights into land–ocean carbon flux dynamics. Here, we analyse two replicate coral cores collected from Singapore, where we collected ~ monthly measurements over 2 years of CDOM absorption spectra, DOC concentration, and estimated tDOC concentration based on carbon stable isotopes (Zhou et al., 2021). We show that coral luminescence G/B can be used as a quantitative proxy to estimate tDOC concentration as well as the full CDOM absorption spectrum, demonstrating that this proxy can provide considerable insights into coastal carbon cycling in the tropics.

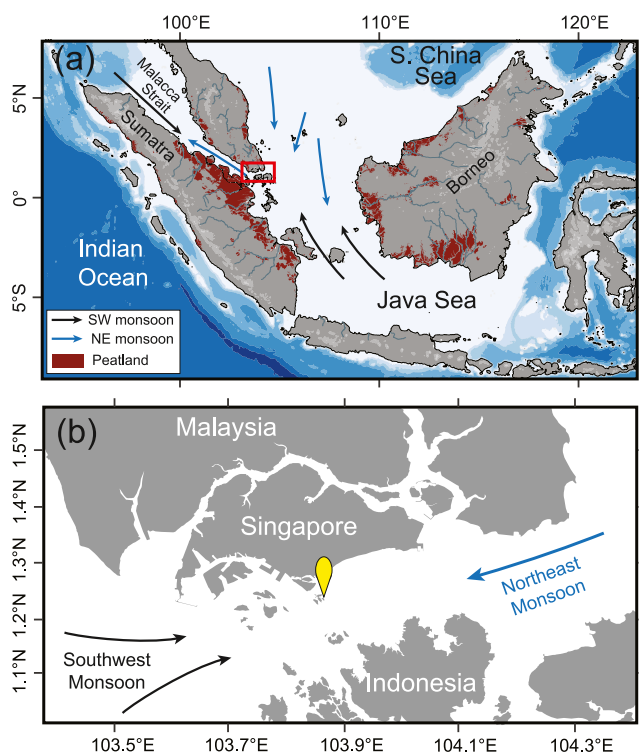


Figure 1. (a) Map of our study region showing the location of tropical peatlands and seasonal monsoon wind directions. During the northeast monsoon months, the currents transport waters from the South China Sea to our study region. During the southwest monsoon months, the currents reverse, transporting waters with inputs from tropical peatlands located on the east coast of Sumatra to our study site. Red rectangle indicates the region shown in panel (b). (b) Site for time series sampling and coral core collection in the Singapore Strait (yellow marker).

2. Material and Methods

2.1. Study Site and Coral Core Collection

The Singapore Strait is located in the central Sunda Shelf Sea (Figure 1) where water depths are mostly <50 m, and strong tidal currents fully mix the water column (Mayer & Pohlmann, 2014). The annual net circulation runs from the South China Sea into the Indian Ocean via the Malacca Strait owing to the pressure gradient between the South China Sea and the Andaman Sea that results from the basin-wide response to the monsoon winds. However, the monsoon system causes the direction of ocean currents to reverse seasonally. During the peak southwest (SW) monsoon months from June to August, the current flows eastward from the coast of Sumatra through the Singapore Strait (van Maren & Gerritsen, 2012). Sumatra harbors the largest deposits of peat in Southeast Asia (Page et al., 2011) and the rivers draining these peatlands (which carry up to $5,000 \mu\text{mol l}^{-1}$ DOC) are one of the most significant sources of tDOC to Southeast Asian coastal waters (Alkhatib et al., 2007; Baum et al., 2007; Rixen et al., 2008; Wit et al., 2018). The seasonally reversing currents thus result in seasonally high concentrations of tDOC and terrigenous CDOM in the Singapore Strait (Martin et al., 2021; Zhou et al., 2021).

One plug core was collected from the main growth axis of each two massive *Porites* spp. corals (KU-K and KU-L) off Kusu Island in the Singapore Strait ($1.226^\circ\text{N } 103.860^\circ\text{E}$, Figure 1) at 2–3 m depth in November 2020, using an underwater electric drill with a 3 cm diameter, 30 cm length diamond bit core barrel. The cores were cleaned with water and sliced (~ 0.7 cm thick) using a rotary saw, and then further cleaned for 48 hr in a 1:4 dilution of household bleach (NaOCl , 3%–7% reactive chlorine) and sonicated in deionized water for a total of 30 min (water changed every 10 min); this removes contaminants and thereby increases the luminescence intensity but without altering the luminescence ratio of green to blue wavelengths (Nagtegaal et al., 2012). The KU-K plug core (hereafter KU-K) measures ~ 13 cm in length and has 11 visible couplets of dark and light bands. The KU-L plug core (hereafter KU-L) measures ~ 7 cm in length and has seven visible couplets of dark and light bands. The seasonal timing of luminescent band formation in Singa-

pore was previously ascertained through alizarin staining and repeated subsampling of tagged colonies (Tanzil et al., 2016). The dark bands in true color images (bright bands in luminescence images) represent coral skeletal growth during the SW monsoon period of high tDOC influx (Tanzil et al., 2016; Zhou et al., 2021). Here, we subsampled 4.8 cm of the KU-K and 3.0 cm of the KU-L cores, covering the growth period from the end of the SW monsoon in 2017 to core collection in November 2020.

2.2. Kusu Seawater Biogeochemical Sampling

Biogeochemical sampling was conducted at Kusu once or twice per month at 5 m depth from October 2017 to November 2020. The collection, preservation, and analysis of water samples are described in detail in Zhou et al. (2021), and are only briefly mentioned here and below (Section 2.3.1). Profiles of salinity and temperature were measured using a FastCTD Profiler (Valeport Ltd). Water samples for CDOM, DOC, and $\delta^{13}\text{C}_{\text{DOC}}$ measurements were collected using a Niskin bottle and immediately filtered onboard through a pre-rinsed 47 mm diameter, $0.22 \mu\text{m}$ pore-size polyethersulfone membrane filter (Supor, Merck Millipore) in an in-line filter housing connected to a peristaltic pump.

2.3. Experimental Methods

2.3.1. Water Sample Analysis

CDOM absorption spectra were measured on a Thermo Evolution 300 dual-beam spectrophotometer in a 10-cm quartz cuvette from 230 to 900 nm. Ultrapure deionized water ($18.2 \text{ M}\Omega \text{ cm}^{-1}$) was used as the reference. The CDOM absorbance (A_λ) was converted to absorption coefficient (a_λ) using:

$$a_\lambda = 2.303 \times (A_\lambda / l) \quad (1)$$

where, a_λ and A_λ are, respectively, the absorption coefficient and the absorbance at wavelength λ , and l is the cuvette length in m. We refer to CDOM absorption at wavelength λ as $a_{\text{CDOM}}(\lambda)$. SUVA_{254} is the specific UV absorbance at 254 nm and was calculated from the absorbance at 254 nm and the DOC concentration (Weishaar et al., 2003). The CDOM spectral slope $S_{275-295}$ and spectral slope ratio S_R (the ratio of $S_{275-295}$ to the spectral slope between 350 and 400 nm) were calculated as in Helms et al. (2008) (Helms et al., 2008). DOC samples (30 ml) were acidified with 100 μl 50% v/v H_2SO_4 and analyzed on a Shimadzu TOC-L system. Potassium hydrogen phthalate was used for calibration and accuracy was monitored using deep-sea certified reference material from the University of Miami, USA with a long-term reproducibility of $48.0 \pm 3.9 \mu\text{mol L}^{-1}$. The $\delta^{13}\text{C}_{\text{DOC}}$ samples were measured at the Jan Veizer Stable Isotope Laboratory, University of Ottawa, Canada, using an OI Analytical Aurora Model 1030W TOC Analyzer interfaced to a Finnigan Mat DeltaPlusXP isotope ratio mass spectrometer with a long-term reproducibility of $\pm 0.4 \%$. The spectral slope ratios were published in Martin et al., 2021, while the remaining parameters (water temperature, salinity, CDOM absorption, $S_{275-295}$, SUVA_{254} , DOC concentration, $\delta^{13}\text{C}_{\text{DOC}}$) were published in Zhou et al., 2021. Here, we used monthly averaged values of the water measurements for comparison against coral data. We used the higher-resolution $a_{\text{CDOM}}(350)$ data *only* for age-depth model development.

2.3.2. Coral Core Luminescence, $\delta^{18}\text{O}$ and Sr/Ca Measurements

Luminescence was measured parallel to the sampling track for Sr/Ca and $\delta^{18}\text{O}$ measurements. The cleaned KU-K and KU-L sections were scanned under ultraviolet light (365 nm) using spectral line scanning on an Avaatech XRF core scanner at the Asian School of the Environment following Grove et al. (2010) and Tanzil et al. (2016). The line scan camera records luminescence emission while the light source and recording camera progress down the coral section as a single unit, scanning multiple lines that are stitched together to produce a continuous core section image. The incoming light from the sample is split into three wavelength bands (red, green, and blue) by a dichroic RGB beam splitter prism and recorded by separate sensors. Coral luminescence green-to-blue ratio (hereafter referred to as coral G/B) measurements were obtained along the main growth axis for a 2 mm wide track at a resolution of 143 pixels cm^{-1} ($\sim 0.07 \text{ mm}$), with wavelength bands of green: 525–575 nm and blue: 425–475 nm. Ratioing to the blue band normalizes for changes to the luminescence signal resulting from down-core changes in coral density and architecture (Grove et al., 2010). Coral samples for Sr/Ca and $\delta^{18}\text{O}$ were drilled continuously at 1 mm resolution for Sr/Ca and $\delta^{18}\text{O}$ measurements. Further details of these measurements have been provided in the Supplementary Information.

2.4. Theory and Calculation

2.4.1. Estimating Terrigenous Dissolved Organic Carbon (tDOC) Concentration

Zhou et al. (2021) used a two-endmember mixing model to estimate the concentration of tDOC from our measured time series of DOC concentration and $\delta^{13}\text{C}_{\text{DOC}}$ in the Singapore Strait, and the estimated endmember $\delta^{13}\text{C}_{\text{DOC}}$ values for peatland-derived DOC (i.e., pure tDOC) and for marine DOC. The $\delta^{13}\text{C}_{\text{DOC}}$ endmember values (mean $\pm 1\sigma$ uncertainty) were taken as $-29 \pm 1\%$ for peatland DOC, based on data from Sumatra, Borneo, and peninsular Malaysia, and as $-21.88 \pm 0.79\%$ for autochthonous marine DOC, based on the Singapore Strait data during the late NE monsoon and inter-monsoon (late February–March, when the Singapore Strait receives waters from the open South China Sea). The tDOC concentration for each sampling date was calculated by Zhou et al. (2021) as follows:

In our coastal sites, the measured DOC concentration ($[\text{DOC}]_{\text{meas}}$) is the sum of the terrigenous fraction ($[\text{tDOC}]$) and the marine fraction ($[\text{mDOC}]$):

$$[\text{DOC}]_{\text{meas}} = [\text{tDOC}] + [\text{mDOC}] \quad (2)$$

Also, the measured concentration of DO^{13}C ($[\text{DO}^{13}\text{C}]_{\text{meas}}$) is the sum of the terrigenous fraction ($[\text{DO}^{13}\text{C}]_{\text{tDOC}}$) and the marine fraction ($[\text{DO}^{13}\text{C}]_{\text{mDOC}}$):

$$[\text{DO}^{13}\text{C}]_{\text{meas}} = [\text{DO}^{13}\text{C}]_{\text{tDOC}} + [\text{DO}^{13}\text{C}]_{\text{mDOC}} \quad (3)$$

The $[\text{DO}^{13}\text{C}]_{\text{meas}}$ is calculated from the measured DOC and $\delta^{13}\text{C}_{\text{DOC}}$ as:

$$[\text{DO}^{13}\text{C}]_{\text{meas}} \approx [\text{DOC}]_{\text{meas}} R_{\text{meas}} \quad (4)$$

where R_{meas} is the measured carbon isotope ratio, calculated as:

$$R_{\text{meas}} = (\delta^{13}\text{C}_{\text{DOCmeas}}(\text{‰}) \div 1000 + 1) R_{\text{VPDB}} \quad (5)$$

The $[\text{DO}^{13}\text{C}]_{\text{tDOC}}$ is approximated as:

$$[\text{DO}^{13}\text{C}]_{\text{tDOC}} \approx [\text{tDOC}] R_{\text{tDOC}} \quad (6)$$

where R_{tDOC} is the carbon isotope ratio of tDOC, and calculated using the riverine endmember of carbon isotopic composition of DOC:

$$R_{\text{tDOC}} = (\delta^{13}\text{C}_{\text{DOCriver}}(\text{‰}) \div 1000 + 1) R_{\text{VPDB}} \quad (7)$$

Similarly, R_{mDOC} is the carbon isotope ratio of marine DOC and is calculated in the same fashion from the marine DOC (mDOC) $\delta^{13}\text{C}$ endmember value. Equation 2 can then be rewritten as:

$$[\text{DOC}]_{\text{meas}} R_{\text{meas}} = [\text{tDOC}] R_{\text{tDOC}} + [\text{mDOC}] R_{\text{mDOC}} \quad (8)$$

where R_{mDOC} is the carbon isotope ratio of marine DOC, calculated using the marine endmember of carbon isotopic composition of DOC.

Solving Equation 2 and Equation 8 returns the concentration of terrigenous DOC.

2.4.2. Coral Age-Depth Model

The age–depth models were created using coral G/B and our measured $a_{\text{CDOM}}(350)$, which has a pronounced SW monsoon peak (Zhou et al., 2021). Seasonal coral G/B at this site is distinct and cyclically reproducible between colonies from the same location, while skeletal density variations show a lack of discernible annual patterns (Tanzil et al., 2016). Sixty-three $a_{\text{CDOM}}(350)$ measurements were made at Kusu from October 2017 to October 2020, which provides a less ambiguous seasonal marker than water temperature or salinity (Supp. Figure 1). QAnalyze software was used to peak-align the 2018 and 2019 SW monsoon peaks in $a_{\text{CDOM}}(350)$ with corresponding peaks in coral G/B, providing an age–depth model for each core, yielding a growth rate of 16 mm year⁻¹ for KU-K and 10 mm year⁻¹ for KU-L. To further validate our age–depth model, we compared our temperature and salinity time series data to the coral Sr/Ca and $\delta^{18}\text{O}$ measurements.

2.4.3. Reconstructing Full CDOM Absorption Spectra From Coral G/B

We used two different methods to test whether coral G/B can be used to reconstruct full CDOM absorption spectra. In Method 1, we used coral G/B to reconstruct CDOM absorption at 300 and 400 nm, set the absorption at 700 nm to 0 m⁻¹ (Green & Blough, 1994) and fit a first-order exponential curve (Bricaud et al., 1981; Grunert et al., 2018) through the three points. We also test a second approach (Method 2), in which we used coral G/B to reconstruct absorption at wavelength 350 and took the average of the measured water CDOM spectral slope over the range 300–550 nm, and calculated the rest of the absorption spectrum following (Bricaud et al., 1981):

$$a_{\lambda} = a_{\lambda_{\text{ref}}} e^{-S(\lambda - \lambda_{\text{ref}})} \quad (9)$$

where a_{λ} and $a_{\lambda_{\text{ref}}}$ are the absorption coefficients (m⁻¹) at wavelengths λ and λ_{ref} , λ_{ref} is the reference wavelength (350 nm in our case), and S is the spectral slope between 300 and 550 nm.

3. Results

3.1. Monsoon-Driven Seasonality of tDOC in the Singapore Strait

As previously described (Martin et al., 2021; Zhou et al., 2021), the Singapore Strait experiences a large input of tDOC and terrigenous CDOM during the SW monsoon (mid-May to mid-September, Figure 2), when currents transport peatland-influenced waters from the east coast of Sumatra through the Singapore Strait. This results in:

1. A drop in salinity from ~ 33 to ~ 30 ,
2. Spikes in DOC concentration ($>80 \mu\text{mol kg}^{-1}$), in CDOM absorption ($a_{\text{CDOM}}(350) > 0.5 \text{ m}^{-1}$) and SUVA_{254} ($>1.5 \text{ L mg}^{-1} \text{ m}^{-1}$),
3. Large decreases in CDOM spectral slope $S_{275-295}$ ($<0.020 \text{ nm}^{-1}$) and in $\delta^{13}\text{C}_{\text{DOC}}$ ($<-24 \text{ ‰}$),
4. And high estimated tDOC concentrations ($>20 \mu\text{mol kg}^{-1}$).

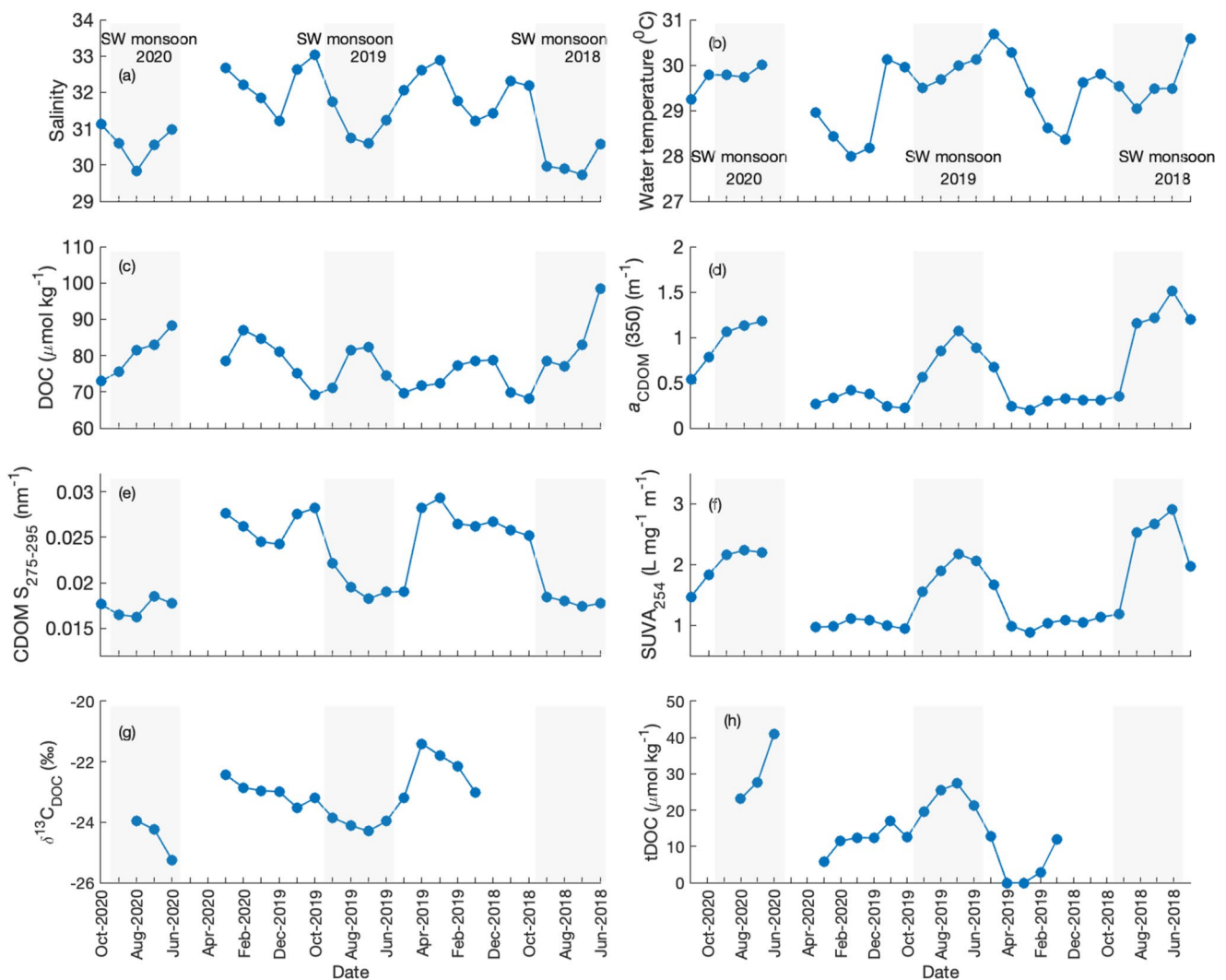


Figure 2. Monthly average biogeochemical data at Kusu Island (for full time series with all individual data, see Martin et al., 2021 and Zhou et al., 2021). Note: The X-axis goes from younger-to-older from left-to-right to facilitate comparison with the coral data. (a) Salinity indicates a large input of freshwater during the SW monsoon (gray shading), while (b) water temperature shows limited seasonal variation with lowest temperature during the NE monsoon. (c) The bulk dissolved organic carbon (DOC) pool shows clear peaks during the southwest (SW) and northeast monsoon, but (d–f) the chromophoric dissolved organic matter (CDOM parameters and (g) $\delta^{13}\text{C}_{\text{DOC}}$ show that a large input of terrigenous dissolved organic matter only takes place during the SW monsoon. (h) Concentration of terrigenous dissolved organic carbon (tDOC) as calculated from the DOC concentration and the $\delta^{13}\text{C}_{\text{DOC}}$ data. The tDOC for March 2019 and April 2019 are less than zero, which is a result of using a single, fixed marine endmember value for $\delta^{13}\text{C}_{\text{DOC}}$ (from late February–March).

The early NE monsoon (December–January), when currents begin to transport open South China Sea water to the Singapore Strait, is also the season with most rainfall in Singapore and southern Malaysia. At this time, there is a smaller drop in salinity from 33 to 31, and lowest annual water temperatures of 28°C. DOC concentration increases to $\sim 80 \mu\text{mol kg}^{-1}$, comparable to the SW monsoon, but indicators of tDOM input show much smaller changes than during the SW monsoon: $a_{\text{CDOM}}(350)$ is $< 0.5 \text{ m}^{-1}$, $\text{SUVA}_{254} \sim 1 \text{ L mg}^{-1} \text{ m}^{-1}$, $\delta^{13}\text{C}_{\text{DOC}} \sim -22.5\text{‰}$, and $S_{275-295} \sim 0.025 \text{ nm}^{-1}$. The estimated tDOC concentration is therefore consistently $< 20 \mu\text{mol kg}^{-1}$.

3.2. Coral Age-Depth Model

Following the results from peak-aligning we use the KU-K section that grew from January 2018 to February 2020, and the KU-L section that grew from October 2017 to November 2019 for analysis in this study. These sections cover both the 2018 and 2019 SW monsoons, represented by bright layers in the coral luminescence images (Figures 3a and 3b), dark brown colored bands in the true-color images (Figures 3c and 3d) and peaks in coral G/B (Figures 3e and 3f). The $a_{\text{CDOM}}(350)$ peak-aligned coral G/B values are shown in Figure 3g.

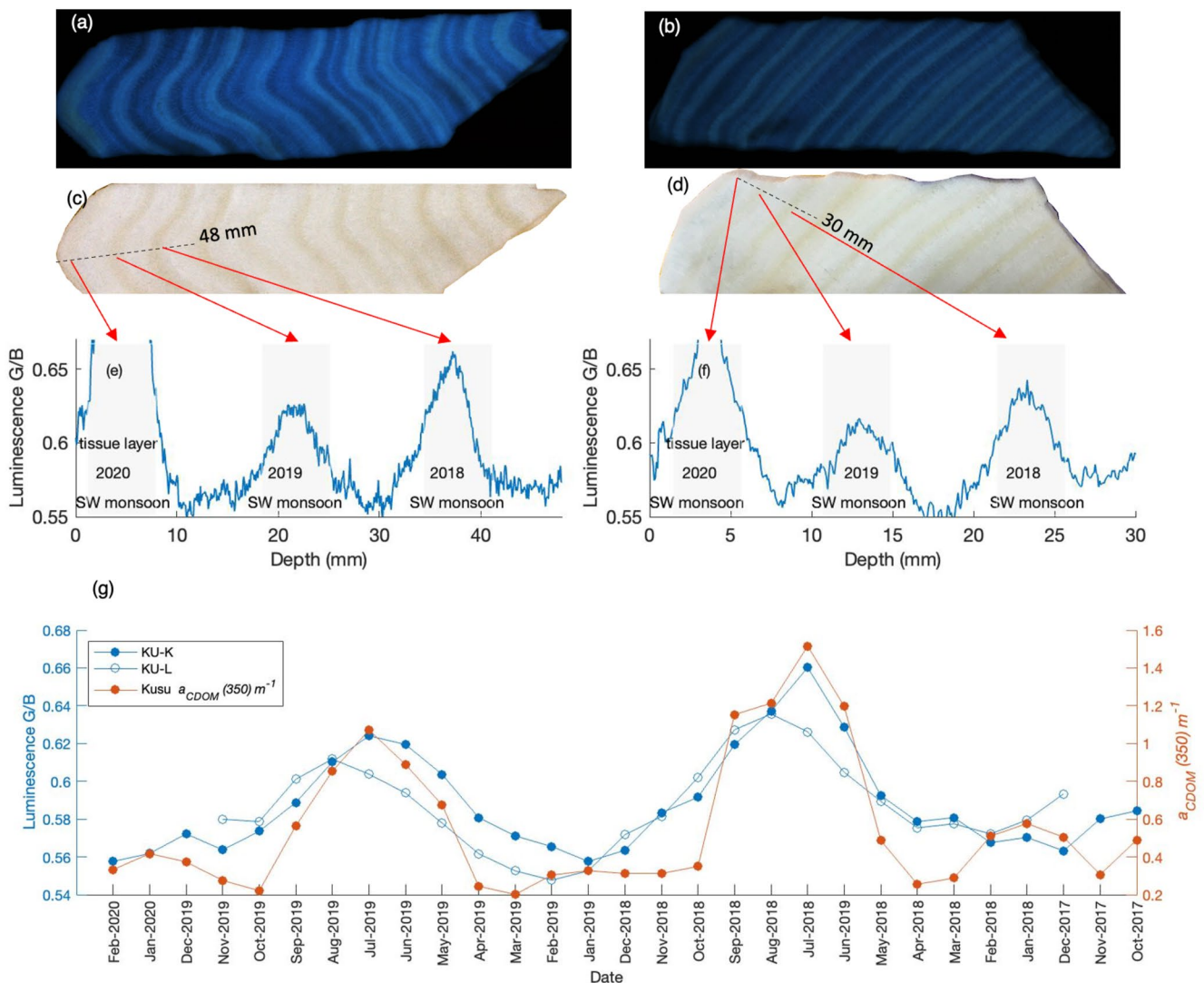


Figure 3. Coral luminescence green-to-blue ratio (coral G/B) measurements. Luminescence (under ultraviolet excitation) and true-color images of coral plug cores (a, c) KU-K and (b, d) KU-L from Kusu Island. Dashed black lines in (c, d) indicate the growth axis along which coral G/B was quantified (e, f) The raw coral G/B measurements have been plotted against core depth. The core top “tissue layers” show very high coral G/B and are omitted from our analysis. The approximate timing of the 2019 and 2018 SW monsoon periods are marked. (g) A monthly resolution age model was developed for the coral G/B by peak-aligning with measured $a_{\text{CDOM}}(350)$.

We then compared the measured temperature and salinity data to the corresponding coral Sr/Ca and $\delta^{18}\text{O}$ data according to our agedepth model (Supp. Figure 2). In both cores, high water temperature coincides with low Sr/Ca, and high salinity coincides with high $\delta^{18}\text{O}$, which provides additional, independent validation of our age model.

3.3. Reconstructing tDOC and CDOM Using Coral G/B as a Proxy

To test whether coral G/B ratios can track tDOC in coastal waters we compared coral G/B ratios with bulk DOC (which includes both the marine and terrigenous components of DOC; Figure 4a), with $\delta^{13}\text{C}_{\text{DOC}}$ (where more negative values indicate a greater contribution from terrigenous DOC to the bulk DOC pool; Figure 4b), and with our calculated tDOC concentration (Figures 4c and 4d). The coral G/B ratio varied between 0.58 and 0.68 with distinct peaks in the SW monsoon, which coincided with the SW monsoon peak in bulk DOC (Figure 4a). However, the coral G/B did not reflect the NE monsoon peak in bulk DOC, and coral G/B was therefore only poorly correlated with bulk DOC (KU-K $R = 0.21$; KU-L $R = 0.3$; Figure 4a). Coral G/B instead correlated well with $\delta^{13}\text{C}_{\text{DOC}}$ (KU-K $R = -0.60$; KU-L $R = -0.86$; Figure 4b) and with calculated tDOC concentration (KU-K $R = 0.64$; KU-L $R = 0.90$; Figures 4c and 4d). We then used the two regression models from Figure 4c to reconstruct tDOC from the coral G/B records; this reconstruction has an RMSE of $\pm 6.3 \mu\text{mol kg}^{-1}$. Our reconstructed tDOC time series varies from 3 to 37 $\mu\text{mol kg}^{-1}$ between October 2017 and February 2020, with both cores indicating higher tDOC concentrations during the 2018 SW monsoon than in 2019 (Figure 4d).

Moreover, coral G/B was strongly correlated ($R > 0.6$) with monthly average CDOM absorption at every wavelength between 230 and 550 nm (Figure 5a), which essentially covers the full wavelength spectrum of CDOM absorption. At wavelengths greater than 550 nm, monthly mean CDOM absorption was always $< 0.01 \text{ m}^{-1}$ (Figure 5b).

CDOM absorption and spectral slope parameters are a valuable way of comparing CDOM variability in different environments (Vantrepotte et al., 2015) in addition to providing independent information on the composition and biogeochemical processing of CDOM (e.g., Helms et al., 2008; Weishaar et al., 2003). Of the CDOM parameters, coral G/B was most strongly correlated with $a_{\text{CDOM}}(350)$ (KU-K $R = 0.91$; KU-L $R = 0.83$; Figure 6a) and with SUVA_{254} (KU-K $R = 0.89$; KU-L $R = 0.83$; Figure 6b), which are good tracers of terrigenous DOM in this region (Martin et al., 2018, 2021; Zhou et al., 2021). Coral G/B was also quite strongly correlated with the CDOM spectral slope parameters $S_{275-295}$ (KU-K $R = -0.78$; KU-L $R = -0.76$; Figure 6c) and slope ratio (KU-K $R = -0.78$; KU-L $R = -0.73$; Figure 6d), although these correlations are weaker than for $a_{\text{CDOM}}(350)$ and SUVA_{254} because $S_{275-295}$ and the slope ratio showed little difference between the 2018 and 2019 SW monsoons. SUVA_{254} is emerging as a key measure to understand and model tDOC in the ocean (Anderson et al., 2019) and we found that coral G/B can also be used as a proxy to reconstruct SUVA_{254} , with low RMSE values of $\pm 0.34 \text{ L mg}^{-1} \text{ m}^{-1}$ (Figures 6e and 6f).

3.4. Reconstructing Full CDOM Spectra Using Coral G/B as a Proxy

We tested two methods for reconstructing the full CDOM absorption spectrum: Method 1 simply reconstructs absorption at a limited number of points and estimates the full spectrum by fitting an exponential curve to the reconstructed points, while Method 2 requires an estimate of the CDOM spectral slope from field measurements. We find that both methods provide similarly accurate reconstructions of the CDOM absorption spectrum, as measured by the absolute and percentage RMSE between reconstructed and measured absorption at each wavelength, although Method 1 may perform very slightly better (Figure 7). The linear models for reconstruction of absorption spectra, spectral slope measurements (from 300 to 550 nm) and plots of measured and reconstructed spectra are shown in Figures S3–S5 in Supporting Information S1.

4. Discussion

4.1. tDOC Source and Seasonal Variability

At our study site, we use tDOC estimates previously calculated from a carbon isotope mass balance and CDOM parameters as measured by Zhou et al., 2021. The terrigenous organic carbon delivered by peatland-draining

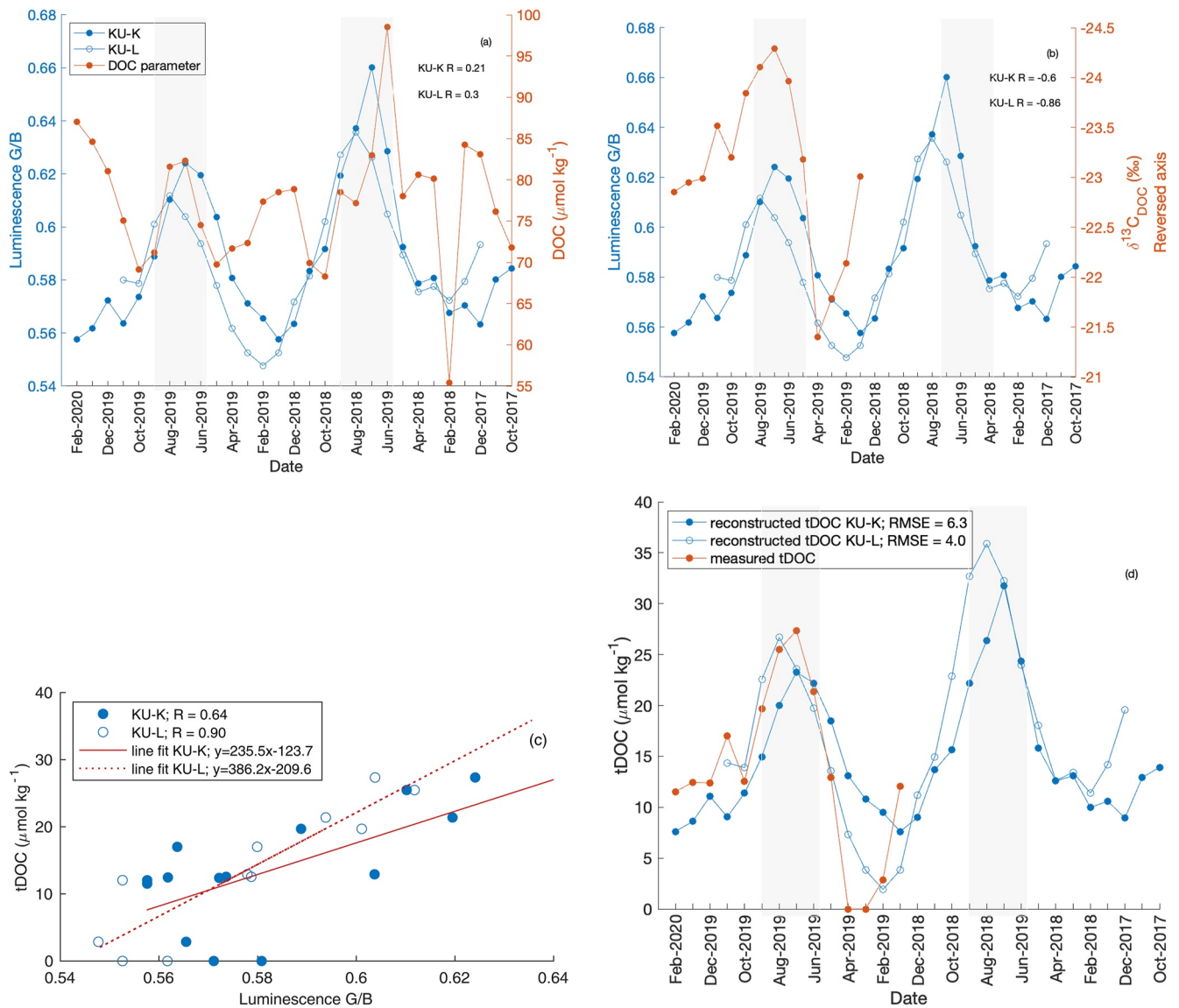


Figure 4. Terrigenous dissolved organic carbon (tDOC) reconstruction using coral luminescence green-to-blue ratio (coral G/B) measurements. (a) Bulk dissolved organic carbon (DOC) concentration, (b) $\delta^{13}\text{C}_{\text{DOC}}$, (c) coral G/B versus tDOC and (d) reconstructed tDOC. tDOC was calculated using the bulk DOC concentration and $\delta^{13}\text{C}_{\text{DOC}}$ measurements using an isotope mass balance approach. The relationship between measured coral G/B and tDOC has been used to reconstruct tDOC going back to October 2017. The measured tDOC and reconstructed tDOC values show RMSE values of $6.3 \mu\text{mol kg}^{-1}$ during the overlapping period from January 2019 to February 2020.

ivers to the Sunda Sea Shelf is overwhelmingly in the form of DOC (typically >95%) rather than POC (Alkhatib et al., 2007; Moore et al., 2011; Müller et al., 2015), so that our proposed proxy for tDOC captures the bulk of the terrigenous carbon input to the Sunda Shelf Sea. Coastal waters in the Sunda Shelf Sea receive relatively high tDOC inputs year-round (Sanwlani et al., 2022; Wit et al., 2018). Although year-to-year variation in rainfall may cause some variation in the tDOC flux from peatlands, the seasonal variability in tDOC seen in Singapore is caused by the monsoonal reversals in ocean currents that bring peatland-influenced waters from the Sumatran coast in the SW monsoon, and open marine waters from the South China Sea during the NE monsoon (Zhou et al., 2021). The large and regular seasonal variation in tDOC at our site therefore make this a particularly suitable location for coral paleoproxy development.

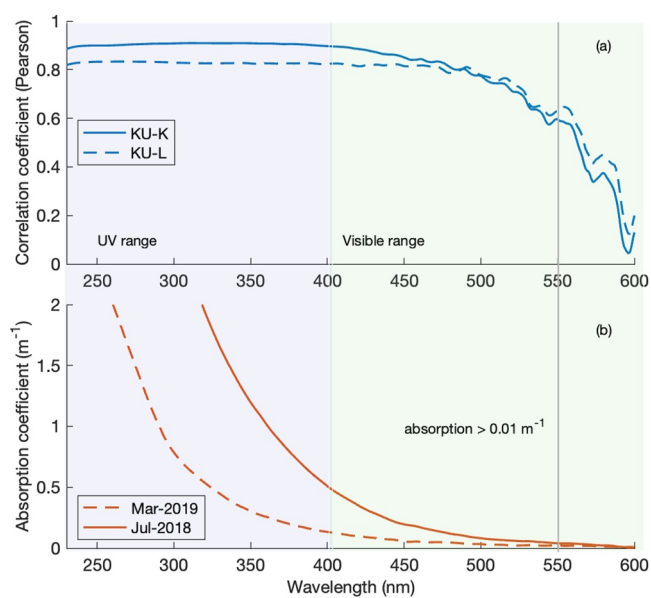


Figure 5. (a) Pearson's correlation coefficient between coral luminescence green-to-blue ratio (coral G/B) and chromophoric dissolved organic matter (CDOM) absorption coefficient at every wavelength between 230 and 600 nm. Strong correlations ($R \geq 0.6$) are seen at all wavelengths up to 550 nm. (b) CDOM absorption spectra measured at Kusu in March 2019 and July 2018, which mark the lowest and highest CDOM absorption measured in our time series, respectively. At wavelengths greater than 550 nm, CDOM absorption was always $< 0.01 \text{ m}^{-1}$, which indicates that coral G/B correlates with CDOM absorption throughout the full CDOM absorption spectrum.

4.2. Coral G/B Is a Sensitive Proxy for tDOC Concentration

Based on a simple linear relationship, we have found that tDOC can be reconstructed from coral G/B measurements with RMSE values of $\pm 6.3 \mu\text{mol kg}^{-1}$. The measured tDOC ranged from 0 to $30 \mu\text{mol kg}^{-1}$ with SW monsoon values of $> 20 \mu\text{mol kg}^{-1}$. From our coral G/B-based reconstruction, we inferred a $10 \mu\text{mol kg}^{-1}$ difference in tDOC between the 2018 and 2019 SW monsoon peaks with a higher concentration in 2018 than 2019. This is also reflected in the measured CDOM parameters, bulk DOC concentration, and salinity, which suggested more freshwater input and higher concentration of tDOM in the Singapore Strait in 2018 compared to 2019 (Martin et al., 2021; Zhou et al., 2021).

Although the $\delta^{13}\text{C}_{\text{DOC}}$ suggests that there might be up to $10 \mu\text{mol kg}^{-1}$ tDOC during the NE monsoon period, the CDOM parameters such as $a_{\text{CDOM}}(350)$ and SUVA_{254} show only small changes at this time (Figure 6). This may indicate that the tDOC pool at this time is inherently less CDOM-rich and less aromatic, or that it has undergone more extensive prior biogeochemical processing that preferentially removed CDOM (e.g., photobleaching; see Helms et al. (2008); Martin et al. (2018)). It is possible that less CDOM-rich and less aromatic-rich tDOM may be less well incorporated by corals. Abiotic precipitation experiments have shown that aragonite does not incorporate DOM indiscriminately, but preferentially incorporates peatland-derived DOM over marine DOM (Kaushal et al., 2020), which may be due to the variable structures of humic-like aromatic ring compounds and available sites for binding with calcium carbonate. However, coral cores also show luminescence due to terrestrial input in regions without peatlands (e.g., Grove et al., 2013), which shows that the coral G/B proxy is not just specific to peatland-derived tDOC.

It is also possible that tDOC during the NE monsoon was overestimated, since it was calculated using a fixed value for the marine endmember $\delta^{13}\text{C}_{\text{DOC}}$, even though marine autochthonous carbon can span a relatively wide range of $\delta^{13}\text{C}$ values (Verwega et al., 2021). It is also not clear whether the peatland tDOC endmember $\delta^{13}\text{C}$ value used by Zhou et al. (2021) is appropriate during the NE monsoon, because the most likely sources of tDOC during the NE monsoon would be local or regional input from the south and east coasts of the Malay Peninsula, where few peatlands are found (Figure 1).

Overall, our data show that coral G/B can be a sensitive proxy for tDOC concentration, and that G/B is not affected by variation in the bulk concentration of marine autochthonous DOC. However, it is possible that coral G/B may be less sensitive to some types of tDOC that are less aromatic, or that have undergone very extensive prior photobleaching. Knowledge of the regional tDOC sources, their CDOM:DOC ratios, and of the possible extent of biogeochemical processing of the tDOC, is therefore advisable before applying this proxy in different regions.

4.3. Coral G/B as a Proxy for CDOM

CDOM parameters measure the absorption of light by DOM at different wavelengths, and DOM that originates from partial degradation of terrigenous vegetation is particularly light-absorbent (Massicotte et al., 2017; Vantrepotte et al., 2015). This is reflected in the high CDOM absorption measured during the SW monsoon (Figure 5). The high correlation of > 0.6 between the measured CDOM absorption and coral G/B ratio is consistent with the corals incorporating humic-like material of terrestrial origin. Of the different measured CDOM parameters, the coral G/B measurements showed highest correlation with $a_{\text{CDOM}}(350)$ and with SUVA_{254} ($R > 0.83$). SUVA_{254} is strongly correlated with aromaticity (Weishaar et al., 2003), which fits well with our understanding of coral luminescence. SUVA_{254} was also recently proposed as a measure to distinguish tDOC pools according to their source and reactivity (especially as photolabile vs. biolabile tDOC) in marine carbon cycle models (Anderson et al., 2019). However, SUVA_{254} data from tropical coastal oceans are scarce, so the fact that this

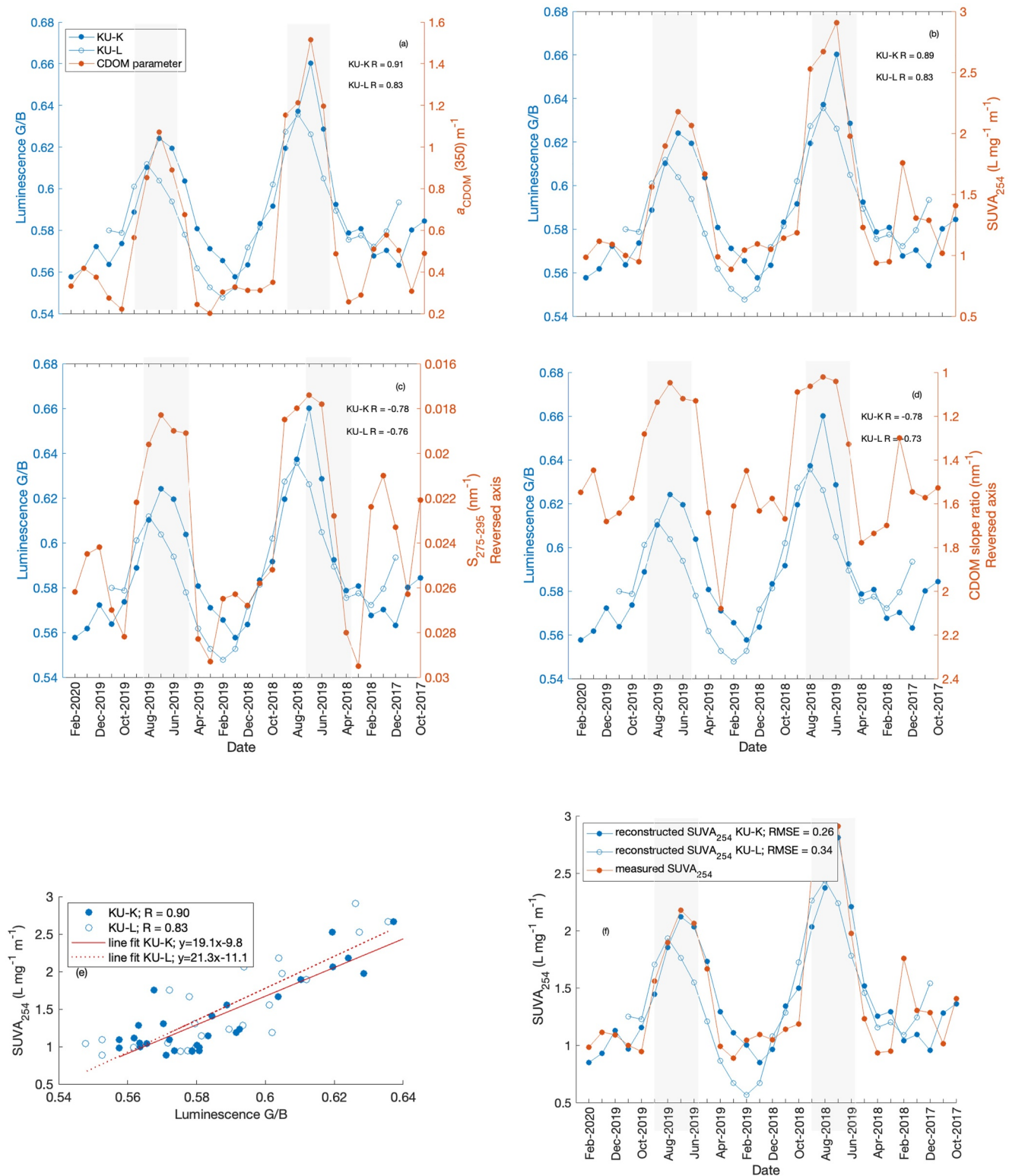


Figure 6. Coral luminescence green-to-blue ratio (coral G/B) has been correlated (Pearson's correlation coefficient) with chromophoric dissolved organic matter (CDOM) parameters relevant for tracing terrigenous dissolved organic matter in the coastal ocean. The highest correlations are seen with (a) $a_{\text{CDOM}}(350)$, and (b) SUVA_{254} , both of which trace terrigenous CDOM concentration in this region. The correlation is slightly lower for the spectral slope parameters (c) $S_{275-295}$ and (d) the slope ratio. Panels (e) and (f) demonstrate that coral G/B can be used to reconstruct SUVA_{254} with low RMSE values of $\pm 0.34 \text{ L mg}^{-1} \text{ m}^{-1}$.

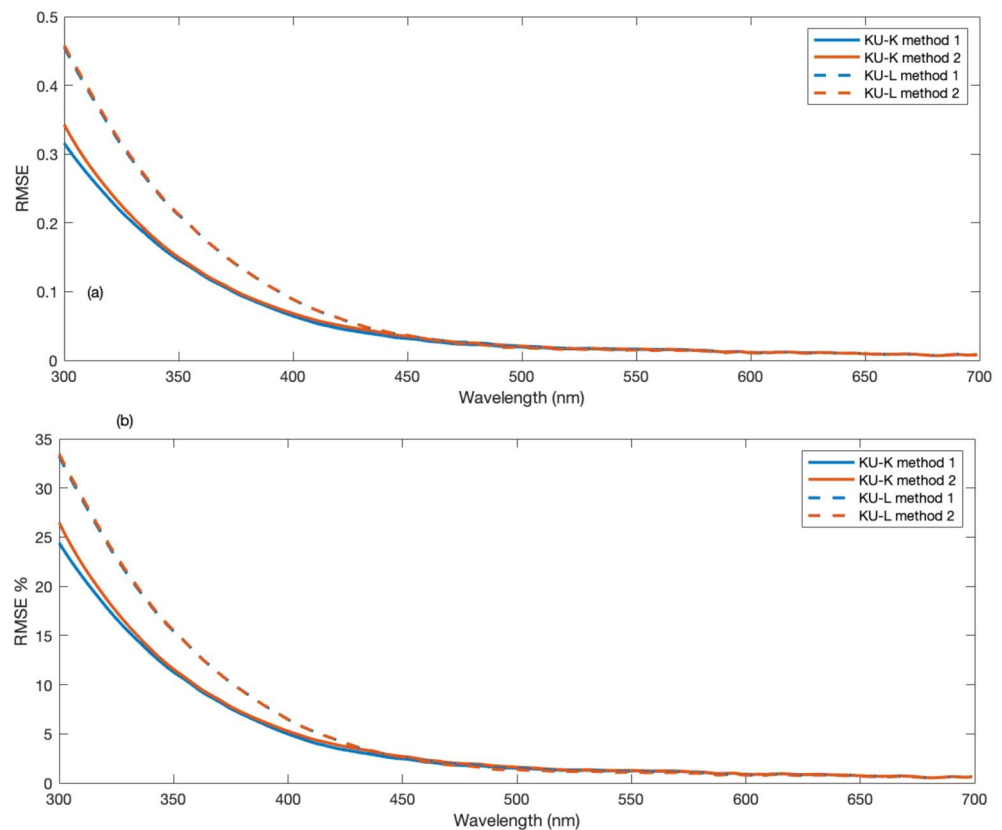


Figure 7. RMSE (300–700 nm) (a) and RMSE percentage (b) against wavelength between the measured chromophoric dissolved organic matter (CDOM) spectra and spectra reconstructed from coral luminescence green-to-blue ratio (coral G/B) using both reconstruction methods. Method 1 uses coral G/B to reconstruct absorption at wavelengths 300 and 400 nm, assumes 0 absorption at 700 nm, and fits a first-order exponential curve through these three points. Method 2 uses coral G/B to reconstruct absorption at wavelength 350 and uses the average CDOM spectral slope between 300 and 550 nm from in-situ CDOM measurements.

parameter can be reconstructed with relatively good accuracy (RMSE of $\pm 0.34 \text{ L mg}^{-1} \text{ m}^{-1}$) from long coral cores may help to inform better marine carbon cycle models.

Compared to CDOM absorption coefficients and to SUVA_{254} , we found that coral G/B was slightly less strongly correlated with the CDOM spectral slope parameters $S_{275-295}$ and slope ratio. In particular, the spectral slope parameters did not reflect the difference between the 2018 and 2019 SW monsoons in tDOM input (as inferred from our in-situ CDOM, DOC, and salinity measurements). While both $S_{275-295}$ and slope ratio are very sensitive measures of the presence of tDOM (Fichot & Benner, 2011; Vantrepotte et al., 2015; Zhou et al., 2021), CDOM spectral slope properties change in a strongly non-linear manner when tDOM mixes with low-CDOM marine DOM, such that even small quantities of terrigenous CDOM initially lead to large changes in spectral slopes, but spectral slopes are then relatively insensitive to further increases in terrigenous CDOM (Stedmon & Markager, 2003). Hence, slope ratios might not be ideal measures of absolute concentration of tDOM and tDOC unless the terrigenous contribution is relatively low. The fact that coral G/B reflects variation in CDOM absorption coefficients and in SUVA_{254} more closely than variation in CDOM spectral slope properties therefore suggests that coral G/B primarily traces the variation in absolute tDOM concentration.

We found that we can reliably reconstruct full CDOM absorption spectra from coral G/B during high CDOM absorption periods (SW monsoon) at our study site. The two methods of CDOM reconstruction that we tested work comparably well. Method 1 fits an exponential curve through reconstructed points and had a slightly lower RMSE compared to Method 2, which uses the CDOM spectral slope from in-situ measurements. Because the CDOM spectral slope might have varied in the past, we suspect that Method 2 may introduce more uncer-

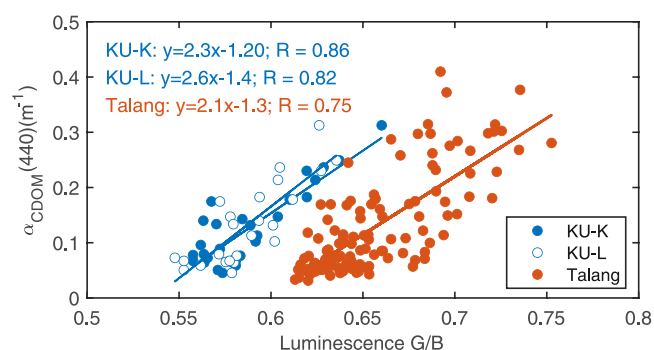


Figure 8. The relationship between coral luminescence green-to-blue ratio (coral G/B) of the KU-K and KU-L cores and measured $a_{\text{CDOM}}(440)$ is compared to the relationship between the Talang coral core G/B measurements and $a_{\text{CDOM}}(440)$ as estimated from satellite remote sensing (Kaushal et al., 2021). The offset on the luminescence axis may suggest that corals preferentially incorporate a relatively labile fraction of the terrigenous dissolved organic matter pool; however, the similarity in slopes suggests that variability within a core nevertheless accurately reflects relative changes in chromophoric dissolved organic matter absorption.

tainty if used for paleo-reconstruction. Therefore, Method 1 provides a simpler approach for the reconstruction of CDOM. Reconstructing the full CDOM absorption spectrum has the potential to provide information about changes in optical water quality, which may contribute to a better understanding of the ecological effects of tDOM fluxes to coastal waters. Anthropogenic increases in the terrigenous CDOM flux to tropical coastal waters has recently been documented (Felgate et al., 2021; Sanwani et al., 2022), and are likely to have led to ecologically relevant reductions in euphotic zone depth and spectral shifts in underwater irradiance (Martin et al., 2021). Such “coastal browning” due to increased terrigenous CDOM flux is thought to have contributed to ecological regime shifts off Norway, including kelp forest collapse (Aksnes et al., 2009; Frigstad et al., 2013), and possibly delaying the North Sea spring phytoplankton bloom (Opdal et al., 2019). Sufficient underwater light availability is critical for coral reef health (Gattuso et al., 2006; Hochberg et al., 2020), and reduced light availability on reefs degrades coral health and ecosystem functioning (Bessell-Browne et al., 2017; Chow et al., 2019; De'ath & Fabricius, 2010). By reconstructing past variation in light absorption by terrigenous CDOM, the coral G/B proxy may help to constrain the extent to which anthropogenic changes in tDOM fluxes have affected the light environment of coral reef ecosystems. We acknowledge that without information about particulate optical properties, a reconstruction of light absorption by tDOM from coral G/B can only provide partial insights

into past variation in the underwater light environment, as light attenuation coefficients can only be estimated properly if the spectra of CDOM and particulate absorption and of particulate backscattering are known (Lee et al., 2005). However, especially if plausible upper and lower ranges of particulate absorption and backscattering spectra are known for a study site, the reconstructed terrigenous CDOM absorption from coral G/B could be used to estimate a likely range for past variation in light attenuation.

4.4. Comparison to Previous Coral Core Calibration

In our previous work, we calibrated G/B ratios of a coral core collected off the coast of Borneo (Talang) with $a_{\text{CDOM}}(440)$ from satellite remote sensing, and also found a strong and linear relationship (Kaushal et al., 2021). Comparing the relationships for coral G/B to $a_{\text{CDOM}}(440)$ between our new, in-situ calibration from Kusu with the previous calibration from the Talang core (Figure 8) reveals that the slopes of linear regressions are statistically indistinguishable since the standard errors (s.e.) of the slopes overlap (KU-K slope = 2.3 ± 0.3 ; KU-L slope = 2.6 ± 0.4 ; Talang slope = 2.1 ± 0.2). Moreover, a regression analysis of the combined data set for all cores showed no significant interaction term between coral G/B and coral core. However, there is a clear offset, with the Talang core having higher G/B for a given seawater $a_{\text{CDOM}}(440)$ value than either of the Kusu cores. This might simply reflect individual differences between coral colonies, although the fact that the two Kusu colonies have nearly identical calibrations might also indicate that there is a consistent difference in the tDOM pool between the sites. The Talang coral is located close to a peatland-draining river, and thus receives tDOM that is likely comparatively fresh and undegraded, given the predominantly conservative mixing pattern of tDOM in Talang coastal waters (Martin et al., 2018). In contrast, the Kusu cores receive tDOM from more distant rivers on Sumatra, and this tDOM has already undergone extensive remineralization and likely loss of CDOM in the coastal ocean prior to reaching the Singapore Strait (Zhou et al., 2021). Coral G/B is caused by the incorporation of a humic- and aromatic-rich fraction of the fluorescent tDOM pool, which itself is a subset of the light-absorbing CDOM pool. It is therefore possible that corals preferentially incorporate a relatively labile fraction of the tDOM pool (perhaps especially to photobleaching), in which case the observed offset between corals might be linked to how rich the terrigenous CDOM pool at each site is in this putatively labile tDOM fraction that incorporated by the corals. Further research is clearly warranted to identify which chemical fractions of the tDOM pool contribute to coral G/B. Importantly, while our results underscore the importance of local calibrations of coral G/B to measured tDOM parameters, the similarity in calibration slopes between both sites indicates that relative variation in terrigenous CDOM might perhaps be inferred from coral G/B even without a local calibration. However, further research and comparison with more coral cores from different sites would be needed to confirm this.

5. Conclusion

Our study demonstrates that monthly resolution tDOC and CDOM variability in tropical coastal oceans can be reconstructed using coral cores. Although this study investigates the relationship between coral G/B, tDOC, and CDOM variability over a short period of 2 years, evidence of coral luminescence persisting over decades to centuries has been shown by previous work (e.g., Grove et al., 2013; Lough, 2007). Thus, our method provides a way to understand long-term drivers of tDOM flux to the coastal ocean. Over these longer time-scales, the tDOM flux maybe driven by multiple factors such as anthropogenic land use change and inter-annual rainfall variability (e.g., Miettinen et al., 2016; Moore et al., 2013; Sanwani et al., 2022). Decoupling the different drivers would benefit from the use of additional tools. A coral multi-proxy approach (e.g., Sr/Ca) can be used to track climate modes that drive inter-annual rainfall variability (e.g., Krawczyk et al., 2020). Further, converting the tDOC concentration to an estimate of carbon flux may require integration with coastal biogeochemical models that can parametrize tDOC input and degradation (Anderson et al., 2019; Mathis, et al., 2022). This information is vital for better quantification of variability in land-to-ocean transfer of carbon, a significant component of the global carbon cycle, as well as to examine the ecological effects of coastal terrigenous CDOM variability.

Data Availability Statement

All data and analysis code are available at <https://doi.org/10.21979/N9/NFIWJV>.

References

- Aksnes, D. L., Dupont, N., Staby, A., Fiksen, Ø., Kaartvedt, S., & Aure, J. (2009). Coastal water darkening and implications for mesopelagic regime shifts in Norwegian fjords. *Marine Ecology Progress Series*, 387, 39–49. <https://doi.org/10.3354/meps08120>
- Alkhatib, M., Jennerjahn, T. C., & Samiaji, J. (2007). Biogeochemistry of the Dumai River estuary, Sumatra, Indonesia, a tropical black-water river. *Limnology & Oceanography*, 52(6), 2410–2417. <https://doi.org/10.4319/lo.2007.52.6.2410>
- Anderson, T. R., Rowe, E. C., Polimene, L., Tipping, E., Evans, C. D., Barry, C. D. G., et al. (2019). Unified concepts for understanding and modelling turnover of dissolved organic matter from freshwaters to the ocean: The UniDOM model. *Biogeochemistry*, 146(2), 105–123. <https://doi.org/10.1007/s10533-019-00621-1>
- Baum, A., Rixen, T., & Samiaji, J. (2007). Relevance of peat draining rivers in central Sumatra for the riverine input of dissolved organic carbon into the ocean. *Estuarine, Coastal and Shelf Science*, 73(3–4), 563–570. <https://doi.org/10.1016/j.ecss.2007.02.012>
- Bessell-Browne, P., Negri, A. P., Fisher, R., Clode, P. L., Duckworth, A., & Jones, R. (2017). Impacts of turbidity on corals: The relative importance of light limitation and suspended sediments. *Marine Pollution Bulletin*, 117(1–2), 161–170. <https://doi.org/10.1016/j.marpolbul.2017.01.050>
- Bricaud, A., Morel, A., & Prieur, L. (1981). Absorption by dissolved organic matter of the sea (yellow substance) in the UV and visible domains. *Limnology & Oceanography*, 26(1), 43–53. <https://doi.org/10.4319/lo.1981.26.1.0043>
- Butman, D. E., Wilson, H. F., Barnes, R. T., Xenopoulos, M. A., & Raymond, P. A. (2015). Increased mobilization of aged carbon to rivers by human disturbance. *Nature Geoscience*, 8(2), 112–116. <https://doi.org/10.1038/ngeo2322>
- Chow, G. S. E., Chan, Y. K. S., Jain, S. S., & Huang, D. (2019). Light limitation selects for depth generalists in urbanised reef coral communities. *Marine Environmental Research*, 147, 101–112. <https://doi.org/10.1016/j.marenvres.2019.04.010>
- Ciais, P., Sabine, C., Bala, G., Bopp, L., Brovkin, V., Canadell, J., et al. (2013). Carbon and other biogeochemical cycles. In *Climate Change 2013: The Physical Science Basis. Contribution of Working Group I to the Fifth Assessment Report of the Intergovernmental Panel on Climate Change* (pp. 465–570). Cambridge University Press.
- Dai, M., Yin, Z., Meng, F., Liu, Q., & Cai, W.-J. (2012). Spatial distribution of riverine DOC inputs to the ocean: An updated global synthesis. *Current Opinion in Environmental Sustainability*, 4(2), 170–178. <https://doi.org/10.1016/j.custos.2012.03.003>
- De'ath, G., & Fabricius, K. (2010). Water quality as a regional driver of coral biodiversity and macroalgae on the Great Barrier Reef. *Ecological Applications*, 20(3), 840–850. <https://doi.org/10.1890/08-2023.1>
- de Wit, H. A., Valinia, S., Weyhenmeyer, G. A., Futter, M. N., Kortelainen, P., Austnes, K., et al. (2016). Current browning of surface waters will be further promoted by wetter climate. *Environmental Science & Technology Letters*, 3(12), 430–435. <https://doi.org/10.1021/acs.estlett.6b00396>
- Drake, T. W., Van Oost, K., Barthel, M., Bauters, M., Hoyt, A. M., Podgorski, D. C., et al. (2019). Mobilization of aged and biolabile soil carbon by tropical deforestation. *Nature Geoscience*, 12(7), 541–546. <https://doi.org/10.1038/s41561-019-0384-9>
- Evans, C. D., Page, S. E., Jones, T., Moore, S., Gauci, V., Laiho, R., et al. (2014). Contrasting vulnerability of drained tropical and high-latitude peatlands to fluvial loss of stored carbon. *Global Biogeochemical Cycles*, 28(11), 1215–1234. <https://doi.org/10.1002/2013GB004782>
- Felgate, S. L., Barry, C. D. G., Mayor, D. J., Sanders, R., Carrias, A., Young, A., et al. (2021). Conversion of forest to agriculture increases colored dissolved organic matter in a subtropical catchment and adjacent coastal environment. *Journal of Geophysical Research: Biogeosciences*, 126(6), e2021JG006295. <https://doi.org/10.1029/2021JG006295>
- Fichot, C. G., & Benner, R. (2011). A novel method to estimate DOC concentrations from CDOM absorption coefficients in coastal waters. *Geophysical Research Letters*, 38(3). <https://doi.org/10.1029/2010GL046152>
- Frigstad, H., Andersen, T., Hessen, D. O., Jeansson, E., Skogen, M., Naustvoll, L.-J., et al. (2013). Long-term trends in carbon, nutrients and stoichiometry in Norwegian coastal waters: Evidence of a regime shift. *Progress in Oceanography*, 111, 113–124. <https://doi.org/10.1016/j.pocean.2013.01.006>
- Gattuso, J.-P., Gentili, B., Duarte, C. M., Kleypas, J. A., Middelburg, J. J., & Antoine, D. (2006). Light availability in the coastal ocean: Impact on the distribution of benthic photosynthetic organisms and their contribution to primary production. *Biogeochemistry*, 3(4), 489–513. <https://doi.org/10.5194/bg-3-489-2006>
- Green, S. A., & Blough, N. V. (1994). Optical absorption and fluorescence properties of chromophoric dissolved organic matter in natural waters. *Limnology & Oceanography*, 39(8), 1903–1916. <https://doi.org/10.4319/lo.1994.39.8.1903>

Acknowledgments

Chen Shuang, Molly Moynihan, Rob Nichols, Kyle Morgan, Kristy Chang, Woo Oon Yee and Chen Yuan assisted with fieldwork and laboratory analysis. We also thank the crew of *Dolphin Explorer*, Francis Yeo, Sapari and Surpato, for enabling the fieldwork. This work was funded by the National Research Foundation, Singapore, Prime Minister's Office, through an NRF–Royal Society Commonwealth Postdoctoral Fellowship to Nikita Kaushal (NRF-SCS-ICFC2017-01) and through the Marine Science Research and Development Programme grants MSRDP-P32 to Patrick Martin and MSRDP-P03 to Jani T.I. Tanzil and Nathalie F. Goodkin, and by the Singapore Ministry of Education through Academic Research Fund Tier 1 grant RG123/18 to Patrick Martin. The coral cores were collected under permit number NP/RP16-156-3b and seawater biogeochemical samples were collected under research permit NP/RP17-044-3 from the Singapore National Parks Board. We thank two anonymous reviewers whose comments considerably improved this manuscript.

- Grove, C. A., Nagtegaal, R., Zinke, J., Scheufen, T., Koster, B., Kasper, S., et al. (2010). River runoff reconstructions from novel spectral luminescence scanning of massive coral skeletons. *Coral Reefs*, 29(3), 579–591. <https://doi.org/10.1007/s00338-010-0629-y>
- Grove, C. A., Zinke, J., Peeters, F., Park, W., Scheufen, T., Kasper, S., et al. (2013). Madagascar corals reveal a multidecadal signature of rainfall and river runoff since 1708. *Climate of the Past*, 9(2), 641–656. <https://doi.org/10.5194/cp-9-641-2013>
- Grunert, B. K., Mouw, C. B., & Ciochetto, A. B. (2018). Characterizing CDOM spectral variability across diverse regions and spectral ranges. *Global Biogeochemical Cycles*, 32(1), 57–77. <https://doi.org/10.1002/2017GB005756>
- Helms, J. R., Stubbins, A., Ritchie, J. D., Minor, E. C., Kieber, D. J., & Mopper, K. (2008). Absorption spectral slopes and slope ratios as indicators of molecular weight, source, and photobleaching of chromophoric dissolved organic matter. *Limnology & Oceanography*, 53(3), 955–969. <https://doi.org/10.4319/lo.2008.53.3.0955>
- Hochberg, E. J., Peltier, S. A., & Maritorena, S. (2020). Trends and variability in spectral diffuse attenuation of coral reef waters. *Coral Reefs*, 39(5), 1377–1389. <https://doi.org/10.1007/s00338-020-01971-1>
- Isdale, P. (1984). Fluorescent bands in massive corals record centuries of coastal rainfall. *Nature*, 310(5978), 578–579. <https://doi.org/10.1038/310578a0>
- Kaushal, N., Sanwlani, N., Tanzil, J. T. I., Cherukuru, N., Sahar, S., Müller, M., et al. (2021). Coral skeletal luminescence records changes in terrestrial chromophoric dissolved organic matter in tropical coastal waters. *Geophysical Research Letters*, 48(8), e2020GL092130. <https://doi.org/10.1029/2020GL092130>
- Kaushal, N., Yang, L., Tanzil, J. T. I., Lee, J. N., Goodkin, N. F., & Martin, P. (2020). Sub-annual fluorescence measurements of coral skeleton: Relationship between skeletal luminescence and terrestrial humic-like substances. *Coral Reefs*, 39(5), 1257–1272. <https://doi.org/10.1007/s00338-020-01959-x>
- Krawczyk, H., Zinke, J., Browne, N., Struck, U., McIlwain, J., O'Leary, M., & Garbe-Schönberg, D. (2020). Corals reveal ENSO-driven synchrony of climate impacts on both terrestrial and marine ecosystems in northern Borneo. *Scientific Reports*, 10(1), 3678. <https://doi.org/10.1038/s41598-020-60525-1>
- Larsen, S., Andersen, T., & Hessen, D. O. (2011). Climate change predicted to cause severe increase of organic carbon in lakes. *Global Change Biology*, 17(2), 1186–1192. <https://doi.org/10.1111/j.1365-2486.2010.02257.x>
- Le Quéré, C., Andres, R. J., Boden, T., Conway, T., Houghton, R. A., House, J. I., et al. (2013). The global carbon budget 1959–2011. *Earth System Science Data*, 5(1), 165–185. <https://doi.org/10.5194/essd-5-165-2013>
- Lee, Z.-P., Du, K.-P., & Arnone, R. (2005). A model for the diffuse attenuation coefficient of downwelling irradiance. *Journal of Geophysical Research*, 110(C2), C02016. <https://doi.org/10.1029/2004JC002275>
- Liu, B., D'Sa, E. J., & Joshi, I. (2019). Multi-decadal trends and influences on dissolved organic carbon distribution in the Barataria Basin, Louisiana from in situ and Landsat/MODIS observations. *Remote Sensing of Environment*, 228, 183–202. <https://doi.org/10.1016/j.rse.2019.04.023>
- Lough, J. M. (2007). Tropical river flow and rainfall reconstructions from coral luminescence: Great Barrier Reef, Australia. *Paleoceanography*, 22(2). <https://doi.org/10.1029/2006PA001377>
- Martin, P., Cherukuru, N., Tan, A. S. Y., Sanwlani, N., Mujahid, A., & Müller, M. (2018). Distribution and cycling of terrigenous dissolved organic carbon in peatland-draining rivers and coastal waters of Sarawak, Borneo. *Biogeosciences*, 15(22), 6847–6865. <https://doi.org/10.5194/bg-15-6847-2018>
- Martin, P., Sanwlani, N., Lee, T., Wong, J., Chang, K., Wong, E., & Liew, S. (2021). Dissolved organic matter from tropical peatlands reduces shelf sea light availability in the Singapore Strait, Southeast Asia. *Marine Ecology Progress Series*, 672, 89–109. <https://doi.org/10.3354/meps13776>
- Massicotte, P., Asmala, E., Stedmon, C., & Markager, S. (2017). Global distribution of dissolved organic matter along the aquatic continuum: Across rivers, lakes and oceans. *Science of the Total Environment*, 609, 180–191. <https://doi.org/10.1016/j.scitotenv.2017.07.076>
- Mathis, M., Logemann, K., Maerz, J., Lacroix, F., Hagemann, S., Chegini, F., et al. (2022). Seamless Integration of the Coastal Ocean in Global Marine Carbon Cycle Modeling. *Journal of Advances in Modeling Earth Systems*, 14(8), e2021MS002789. <https://doi.org/10.1029/2021ms002789>
- Mayer, B., & Pohlmann, T. (2014). Simulation of organic pollutants: First step towards an adaptation to the Malacca Strait. *Asian Journal of Water Environment and Pollution*, 11, 75–86.
- Miettinen, J., Shi, C., & Liew, S. C. (2016). Land cover distribution in the peatlands of Peninsular Malaysia, Sumatra and Borneo in 2015 with changes since 1990. *Global Ecology and Conservation*, 6, 67–78. <https://doi.org/10.1016/j.gecco.2016.02.004>
- Monteith, D. T., Stoddard, J. L., Evans, C. D., de Wit, H. A., Forsius, M., Högåsen, T., et al. (2007). Dissolved organic carbon trends resulting from changes in atmospheric deposition chemistry. *Nature*, 450(7169), 537–540. <https://doi.org/10.1038/nature06316>
- Moore, S., Evans, C. D., Page, S. E., Garnett, M. H., Jones, T. G., Freeman, C., et al. (2013). Deep instability of deforested tropical peatlands revealed by fluvial organic carbon fluxes. *Nature*, 493(7434), 660–663. <https://doi.org/10.1038/nature11818>
- Moore, S., Gauci, V., Evans, C. D., & Page, S. E. (2011). Fluvial organic carbon losses from a Bornean blackwater river. *Biogeosciences*, 8(4), 901–909. <https://doi.org/10.5194/bg-8-901-2011>
- Müller, D., Warneke, T., Rixen, T., Müller, M., Jamahari, S., Denis, N., et al. (2015). Lateral carbon fluxes and CO₂ outgassing from a tropical peat-draining river. *Biogeosciences*, 12(20), 5967–5979. <https://doi.org/10.5194/bg-12-5967-2015>
- Nagtegaal, R., Grove, C. A., Kasper, S., Zinke, J., Boer, W., & Brummer, G.-J. A. (2012). Spectral luminescence and geochemistry of coral aragonite: Effects of whole-core treatment. *Chemical Geology*, 318–319, 6–15. <https://doi.org/10.1016/j.chemgeo.2012.05.006>
- Noacco, V., Wagener, T., Worrall, F., Burt, T. P., & Howden, N. J. K. (2017). Human impact on long-term organic carbon export to rivers. *Journal of Geophysical Research: Biogeosciences*, 122(4), 947–965. <https://doi.org/10.1002/2016JG003614>
- Opdal, A. F., Lindemann, C., & Aksnes, D. L. (2019). Centennial decline in North Sea water clarity causes strong delay in phytoplankton bloom timing. *Global Change Biology*, 25(11), 3946–3953. <https://doi.org/10.1111/gcb.14810>
- Page, S. E., Rieley, J. O., & Banks, C. J. (2011). Global and regional importance of the tropical peatland carbon pool. *Global Change Biology*, 17(2), 798–818. <https://doi.org/10.1111/j.1365-2486.2010.02279.x>
- Rixen, T., Baum, A., Pohlmann, T., Balzer, W., Samiaji, J., & Jose, C. (2008). The Siak, a tropical black water river in central Sumatra on the verge of anoxia. *Biogeochemistry*, 90(2), 129–140. <https://doi.org/10.1007/s10533-008-9239-y>
- Rodriguez-Ramirez, A., Grove, C. A., Zinke, J., Pandolfi, J. M., & Zhao, J. (2014). Coral luminescence identifies the Pacific decadal oscillation as a primary driver of river runoff variability impacting the Southern Great Barrier Reef. *PLoS One*, 9(1), e84305. <https://doi.org/10.1371/journal.pone.0084305>
- Sanwlani, N., Evans, C. D., Müller, M., Cherukuru, N., & Martin, P. (2022). Rising dissolved organic carbon concentrations in coastal waters of northwestern Borneo related to tropical peatland conversion. *Science Advances*, 8(15), eabi5688. <https://doi.org/10.1126/sciadv.abi5688>

- Signorini, S. R., Mannino, A., Friedrichs, M. A. M., St-Laurent, P., Wilkin, J., Tabatabai, A., et al. (2019). Estuarine dissolved organic carbon flux from space: With application to Chesapeake and Delaware bays. *Journal of Geophysical Research: Oceans*, *124*(6), 3755–3778. <https://doi.org/10.1029/2018JC014646>
- Smith, T. J. III, Hudson, H. J., Robblee, M. B., Powell, G. N., & Isdale, P. J. (1989). Freshwater flow from the everglades to Florida Bay: A historical reconstruction based on fluorescent banding in the coral *Solenastrea bournoni*. *Bulletin of Marine Science*, *44*, 274–282.
- Stedmon, C. A., & Markager, S. (2003). Behaviour of the optical properties of coloured dissolved organic matter under conservative mixing. *Estuarine, Coastal and Shelf Science*, *57*(5–6), 973–979. [https://doi.org/10.1016/S0272-7714\(03\)00003-9](https://doi.org/10.1016/S0272-7714(03)00003-9)
- Susic, M., Boto, K., & Isdale, P. (1991). Fluorescent humic acid bands in coral skeletons originate from terrestrial runoff. *Marine Chemistry*, *33*(1–2), 91–104. [https://doi.org/10.1016/0304-4203\(91\)90059-6](https://doi.org/10.1016/0304-4203(91)90059-6)
- Tanzil, J. T. I., Lee, J. N., Brown, B. E., Quax, R., Kaandorp, J. A., Lough, J. M., & Todd, P. A. (2016). Luminescence and density banding patterns in massive *Porites* corals around the Thai-Malay Peninsula, Southeast Asia. *Limnology & Oceanography*, *61*(6), 2003–2026. <https://doi.org/10.1002/lno.10350>
- Thompson, D. M. (2022). Environmental records from coral skeletons: A decade of novel insights and innovation. *Wiley Interdisciplinary Reviews: Climate Change*, *13*(1), e745. <https://doi.org/10.1002/wcc.745>
- Urtizberea, A., Dupont, N., Rosland, R., & Aksnes, D. L. (2013). Sensitivity of euphotic zone properties to CDOM variations in marine ecosystem models. *Ecological Modelling*, *256*, 16–22. <https://doi.org/10.1016/j.ecolmodel.2013.02.010>
- van Maren, D. S., & Gerritsen, H. (2012). Residual flow and tidal asymmetry in the Singapore Strait, with implications for resuspension and residual transport of sediment. *Journal of Geophysical Research*, *117*(C4). <https://doi.org/10.1029/2011JC007615>
- Vantrepotte, V., Danhiez, F.-P., Loisel, H., Ouillon, S., Mériaux, X., Cauvin, A., & Dessailly, D. (2015). CDOM-DOC relationship in contrasted coastal waters: Implication for DOC retrieval from ocean color remote sensing observation. *Optics Express*, *23*(1), 33–54. <https://doi.org/10.1364/OE.23.000033>
- Verwege, M.-T., Somes, C. J., Schartau, M., Tuerena, R. E., Lorrain, A., Oschlies, A., & Slawig, T. (2021). Description of a global marine particulate organic carbon-13 isotope data set. *Earth System Science Data*, *13*(10), 4861–4880. <https://doi.org/10.5194/essd-13-4861-2021>
- Wauthy, M., Rautio, M., Christoffersen, K. S., Forsström, L., Laurion, I., Mariash, H. L., et al. (2018). Increasing dominance of terrigenous organic matter in circumpolar freshwaters due to permafrost thaw. *Limnology and Oceanography Letters*, *3*, 186–198. <https://doi.org/10.1002/lol2.10063>
- Weishaar, J. L., Aiken, G. R., Bergamaschi, B. A., Fram, M. S., Fujii, R., & Mopper, K. (2003). Evaluation of specific ultraviolet absorbance as an indicator of the chemical composition and reactivity of dissolved organic carbon. *Environmental Science & Technology*, *37*(20), 4702–4708. <https://doi.org/10.1021/es030360x>
- Wit, F., Rixen, T., Baum, A., Pranowo, W. S., & Hutahaean, A. A. (2018). The Invisible Carbon Footprint as a hidden impact of peatland degradation inducing marine carbonate dissolution in Sumatra, Indonesia. *Scientific Reports*, *8*(1), 17403. <https://doi.org/10.1038/s41598-018-35769-7>
- Zhou, Y., Evans, C. D., Chen, Y., Chang, K. Y. W., & Martin, P. (2021). Extensive remineralization of peatland-derived dissolved organic carbon and ocean acidification in the Sunda Shelf Sea, Southeast Asia. *Journal of Geophysical Research: Oceans*, *126*(6), e2021JC017292. <https://doi.org/10.1029/2021JC017292>

References From the Supporting Information

- Hathorne, E. C., Gagnon, A., Felis, T., Adkins, J., Asami, R., Boer, W., et al., (2013). Interlaboratory study for coral Sr/Ca and other element/Ca ratio measurements. *Geochemistry, Geophysics, Geosystems*, *14*, 3730–3750. <https://doi.org/10.1002/ggge.20230>
- Kotov, S., & Paelike, H. (2018). QAnalySeries - A cross-platform time series tuning and analysis tool 2018 (pp. PP53D–1230).
- Okai, T., Suzuki, A., Kawahata, H., Terashima, S., & Imai, N. (2002). Preparation of a new geological survey of Japan geochemical reference material: Coral JcP-1. *Geostandards Newsletter*, *26*(1), 95–99. <https://doi.org/10.1111/j.1751-908X.2002.tb00627.x>
- Schrag, D. P. (1999). Rapid analysis of high-precision Sr/Ca ratios in corals and other marine carbonates. *Paleoceanography*, *14*(2), 97–102. <https://doi.org/10.1029/1998PA900025>